Synthesis, Structure and Stability of Phases in the System Li₂O–Pd–O₂

B. L. DUBEY, J. A. GARD, F. P. GLASSER AND A. R. WEST

Department of Chemistry, University of Aberdeen, Meston Walk, Old Aberdeen, Scotland

Li_2PdO_2 and Li_2PdO_3 have been synthesized. Powder X-ray data are reported for both phases. Li_2PdO_2 is body-centered orthorhombic, *Immm*, $a = 3.74_0$, $b = 2.97_5$, $c = 9.35_4$ Å. It is isostructural with Li_2CuO_2, with which it forms a complete series of solid solutions. The crystal structure of Li_2PdO_2 has been determined. it comprises sheets of tetrahedrally coordinated lithium and oxygen atoms, parallel to (001), held together by ribbons of $(PdO_2)_\infty$ in which each palladium atom is coordinated by four oxygen atoms in a rectangular–planar arrangement.

Experimental

Lithium carbonate reacts readily with palladium metal in the presence of oxygen. Li_2PdO_2 and Li_2PdO_3 have been identified as products of the reaction. Li_2PdO_2 is synthesized by heating palladium(II) acetate with Li_2CO_3. The acetate decomposes on heating above ca. 300°C to give fine-grained palladium, which is subsequently oxidized during its reaction with Li_2CO_3. Unfortunately, Li_2CO_3 is so reactive that an inert container could not be found for the reactants: palladium foil was usually used as a container and a substantial excess of Li_2CO_3 was added to compensate. About 100 mg of a mixture of Li_2CO_3 : Pd(Ac)₂ (1.5 : 1) heated in a Pd foil boat at 700–800°C for 24 hr in air gave a nearly pure yield of Li_2PdO_2, judging from powder X-ray patterns. The excess Li_2CO_3 had either evaporated or reacted with the palladium boat.

Li_2PdO_3 was prepared by oxidation of Li_2PdO_2. A sample of Li_2PdO_2 was heated in flowing oxygen at 600°C for 10 days; this yielded a single-phase product.

Between 300 and 500°C, the lithium palladium oxides react readily with atmospheric carbon dioxide. The first signs of attack are a weight gain, blackening, and the appearance of diffuse PdO reflections on X-ray powder photographs, but crystalline Li_2CO_3 is not detected until the latter stages of reaction. Samples heated in this temperature range must be held in a CO_2-free atmosphere to prevent decomposition.

Results

Li₂PdO₂

Single-phase preparations vary in color: made in air at 800°C, the product is yellow-brown, but it is greenish yellow with a slight excess of lithium, and black with excess PdO. These color changes are probably associated with a departure from ideal stoichiometry, but X-ray *d*-spacings remain unchanged. The upper stability limit is 850°C in air, but in a sealed tube filled with oxygen at ambient prior to sealing, it is stable to at least 1050°C. Li_2PdO_2 is insoluble in both water and dilute (2*N*) hydrochloric acid. It grows as small, needle-shaped crystals having high birefringence and parallel extinction in all sections. All refractive indices are greater than 1.78. The unit cell was determined by electron diffraction of single crystals, using evaporated aluminium as an internal standard. Patterns representing numerous sections of the reciprocal lattice were recorded by tilting crystals around various rows of reflections including the b^* and c^* axes; the procedures involved have been fully described elsewhere (*1*). The unit cell was found to be body-centered, and there were no systematically absent reflections other than those with odd values of $(h + k + l)$. The X-ray powder data were indexed and after slight adjustments were made using the measured positions of some of the high angle reflections, the following axial dimensions were obtained: $a = 3.74_0$, $b = 2.97_5$, $c = 9.35_4$ Å. Powder data indexed to 1.03 Å are

given in Table I. Insufficient material was available for a density determination, but packing considerations and the body-centering suggest $Li_4Pd_2O_4$ as the only possible unit cell contents: these give a calculated density of 4.87 g cm^{-1}. A test for piezoelectricity proved negative.

Powder X-ray intensities were measured using a Philips diffractometer equipped with a proportional counter. Each diffraction maximum was integrated over an appropriate interval, and the local background determined, where possible, on both sides of the peak. It was possible to measure intensities for 30 independent reflections. In addition, a total intensity could be measured for five pairs of overlapping reflections. In three of these pairs, each contributing reflection had the same multiplicity. In one of the remaining pairs (004 and 110) the reflections could be resolved for solid solutions containing a small proportion of copper substituted for palladium, and the total intensity for Li_2PdO_2 was divided between (004) and (110) in the ratio observed for the copper-containing solid solutions. Thus, intensities were available for 32 unique and four pairs of reflections. After correction for Lorentz and polarization factors, these intensities were used for the structure determination.

Consideration of the possible space groups—$I222$, $Immm$, $Imm2$ and $I2_12_12_1$—suggested a trial structure which was very close to the final refined version, shown in Fig. 1. The structure has palladium atoms on the lattice points; each palladium is coordinated to four oxygen atoms in a rectangular–planar arrangement. Infinite strips of PdO_2 units run parallel to (100) in the [010] direction; similar strips occur in PdO itself (2, 3). Each lithium atom is coordinated by four oxygen atoms in an irregular tetrahedron. These (LiO_4) tetrahedra are linked by edge sharing to form continuous sheets parallel to the (001) plane. The $(PdO_2)_\infty$ strips connect adjacent sheets by sharing oxygen atoms. This structure fits the centrosymmetric space group $Immm$ with all the atoms lying on special positions.

All structure factors are positive because the heavy palladium atoms are on the lattice points, and the residual

$$[R = 100(\sum |F_{obs} - F_{calc}|/\sum F_{obs})\%]$$

is 22.5% for the palladium atoms alone. Before refinement, the R factor for all atoms in the trial coordinates was 7.9%. At this stage, a less likely alternative model with a and b interchanged was discarded because it gave $R = 19.4\%$. The 32

TABLE I

X-RAY POWDER DIFFRACTION DATA FOR Li_2PdO_2, WITH OBSERVED AND CALCULATED STRUCTURE FACTORS
(F_0 AND F_c)

d (Å)	$h k l$	I	F_0	F_c	d (Å)	$h k l$	I	F_0	F_c
4.68	0 0 2	42	124	140	1.296	1 1 6	5	89	86
3.47	1 0 1	100	187	195	1.264	1 2 3	4	87	87
2.835	0 1 1	26	120	116	1.257[b]	{ 1 0 7	8	140	134
2.395	1 0 3	16	111	107		0 2 4		94	89
2.335[a]	{ 0 0 4	24	113	114	1.236	3 0 1	4	118	119
	1 1 0		113	111	1.219	0 1 7	~1[c]	67	86
2.153	0 1 3	36	189	179	1.209	2 1 5	7	113	105
2.084	1 1 2	35	137	134	1.198	2 0 6	4	119	112
1.870	2 0 0	12	179	178	1.167[b]	{ 0 0 8	5	104	113
1.736	2 0 2	7	105	108		2 2 0		116	127
1.673	1 0 5	7	116	112	1.158	3 0 3	2	84	83
1.650	1 1 4	25	162	161	1.150	3 1 0	2	85	85
1.584	0 1 5	7	120	122	1.130	2 2 2	4	87	88
1.561	2 1 1	10	100	100	1.115[b]	{ 3 1 2	7	91	94
1.559	0 0 6	3	119	132		1 2 5		86	89
1.488	0 2 0	6	166	155	1.076	0 2 6	3	108	104
1.460	2 0 4	5	111	101	1.043[b]	{ 1 1 8	6	83	83
1.418	0 2 2	4	99	99		2 2 4		79	79
1.412	2 1 3	18	157	141	1.037	3 0 5	~1[c]	71	86
1.367	1 2 1	10	124	127	1.032	3 1 4	6	116	114

[a] See text for explanation of derivation of F_0 for these reflections.
[b] $\sum nF_0^2$ divided in proportion to values of nF_c^2.
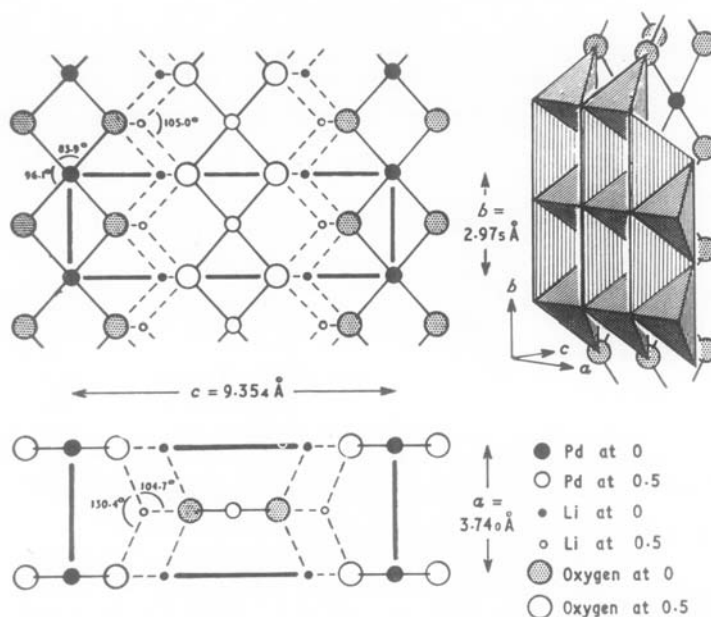[c] Reflections too weak for accurate measurement of I.

FIG. 1. The crystal structure of Li$_2$PdO$_2$ projected on (100) (above left) and (010) (below left); the (PdO$_2$)$_\infty$ strips can be clearly seen on the (100) projection. A perspective view is shown top right of a sheet of (LiO$_4$) tetrahedra, each sharing four edges with adjacent tetrahedra. Two Pd–O strips are shown attached on the far side, but those on the near side are omitted for clarity.

unique reflections were used for least-squares refinement of the z-coordinates of the lithium and oxygen atoms, during which R improved to 4.71 % after four cycles. The oxygen z-coordinate settled quickly to a constant value and that of lithium settled more slowly. At this stage, the observed intensities of the four pairs of reflections were divided in proportion to nF_{calc}^2 for the contributing reflections (where n is the multiplicity factor) giving $R = 4.95\%$. Further refinement is apparently limited by the quality and quantity of the available intensity data, as R increased steadily to 5.16% during three further cycles. The final coordinates were therefore taken as those giving the best R factor, 4.95%, for the 40 F_{obs} values. Exclusion of the (107) and (305) reflections, both of which were too weak for accurate measurement, improved R to 4.33%. The final values of F_{obs} and F_{calc} are given in Table I, and atomic coordinates and isotropic temperature factors in Table II. Interatomic distances and bond angles are given in Table III, where they may be compared with those in PdO and Li$_2$O, calculated from data given in (3) and (4), respectively.

The ideal square–planar arrangement of the (PdO$_2$)$_\infty$ strips is considerably distorted by mutual repulsion between adjacent Pd atoms in

the [010] direction, in spite of the fact that this repulsion is reduced by partial covalency of the Pd–O bonds and by screening due to the oxygen atoms. Pd atoms repel each other more strongly in the [100] direction, where there are no oxygens available for bonding or screening, so the a dimension greatly exceeds b. The [100] edge of each (LiO$_4$) tetrahedron is therefore much longer (3.74 Å) than the other five edges, which are

TABLE II

FRACTIONAL ATOMIC COORDINATES AND ISOTROPIC TEMPERATURE FACTORS FOR Li$_2$PdO$_2$ WITH ESD'S IN PARENTHESES

		x	y	z	$B_{i \cdot o}$
Pd	2 (a)	0	0	0	0.25 (.01)
Li	4 (i)	0	0	0.265 (.013)	2.0 (2.5)
O[b]	4 (j)	0	$\frac{1}{2}$	0.143 (.004)	−1.1 (.8)

[a] The Wyckoff symbols in the space group *Immm* (No. 71) are also given.

[b] Scattering amplitudes for O^{-1}, as given in Ref. (10), were used in the refinement. The negative thermal parameter is physically insignificant and probably reflects inaccuracies in the intensity data.

TABLE III

INTERATOMIC DISTANCES (IN Å) AND ANGLES FOR Li$_2$PdO$_2$, WITH ESD's IN PARENTHESES, COMPARED WITH CORRESPONDING VALUES FOR PdO AND Li$_2$O[a]

Atoms in the (PdO$_2$)$_\infty$ strips			Atoms in the (LiO$_4$) tetrahedra		
	Li$_2$PdO$_2$	PdO		Li$_2$PdO$_2$	Li$_2$O
Pd–O (1 0 0)	2.00 (.03)	2.024	Li–O[b] (1 0 0)	1.88 (.08)	1.997
Pd–Pd [0 1 0]	2.98 (0)	2.668	Li–O[b] (0 1 0)	2.06 (.05)	
Pd–Pd [1 0 0]	3.74 (0)	3.043			
O–O [0 1 0]	2.98 (0)	3.043	O–O [0 1 0]	2.98 (0)	3.261
O–O [1 0 0]	3.74 (0)	3.043	O–O [1 0 0]	3.74 (0)	
O–O [0 0 1]	2.68 (.05)	2.668	O–O	3.12 (.03)	
O–Pd–O ⎱(1 0 0)	83.9° (.9)	82.5°	O–Li–O (1 0 0)	105.0° (3.5)	
O–Pd–O ⎰	96.1° (.9)	97.5°	O–Li–O (0 1 0)	130.4° (3.5)	109.5°
			O–Li–O	104.7° (3.4)	

[a] Calculated from data given in (3) and (4), respectively. The direction or planes in which bonds occur are given where possible.

[b] Li at (0, 0, 0.285) in Li$_2$PdO$_2$ would give equal Li–O distances of 1.990 Å.

either 2.97 or 3.12 Å. Comparing lithium–oxygen distances with that of Li$_2$O (see Table III), Li–O is distinctly shorter in the (100) plane of Li$_2$PdO$_2$, but longer in the (010) plane than in Li$_2$O. These differences may be due to the unequal forces acting on the Li atom in the distorted tetrahedron; on the other hand, the differences may be more apparent than real, as small errors in the F_{obs} values could seriously affect the position found for the Li atom, on account of its very low scattering amplitude. Placing Li at (0,0,0.285) would give equal Li–O distances of 1.990 Å, rather shorter than in Li$_2$O [1.997 Å, calculated from data given in (4)]. A slight difference would be expected, because (LiO$_4$) tetrahedra share four edges with adjacent tetrahedra in Li$_2$PdO$_2$, while in Li$_2$O all six edges are shared.

Li$_2$PdO$_3$

Several investigators have reported the synthesis of Li$_2$PdO$_3$ (5–7), but its properties have not been reported before. X-ray powder data are

TABLE IV

X-RAY POWDER DIFFRACTION DATA FOR Li$_2$PdO$_3$

d (Å)	I	d (Å)	I	d (Å)	I
4.80	vs	2.08	s	1.40	vw
4.40	vvw	1.90	w	1.25	vw
2.51	s	1.60	w	1.20	vw
2.40	m	1.47	vw		

given in Table IV. Its powder pattern is very simple; as previously reported, it is a distorted sodium chloride type. A sample of Li$_2$TiO$_3$ was prepared; comparison of the powder photographs show that the two phases are probably isostructural. Li$_2$TiO$_3$ is a monoclinic distortion of the NaCl structure type (7). However, because several types of distortion exist in this family of compounds, a more exact crystallochemical classification of Li$_2$PdO$_3$ should await an examination of single crystals.

Li$_2$(Pd,Cu)O$_2$ Solid Solutions

Li$_2$CuO$_2$, like Li$_2$PdO$_2$, is reported to be body-centered with $a = 3.659$, $b = 2.862$, $c = 9.386$ Å (9). However, the axial ratios as inferred from these cell dimensions differ considerably from those of Li$_2$PdO$_2$. In order to check whether the two compounds are isostructural, Li$_2$CuO$_2$ was prepared as well as compositions on the join Li$_2$CuO$_2$–Li$_2$PdO$_2$ at 33, 50, and 67 mole% Li$_2$PdO$_2$. After firing, these formed homogeneous solid solutions. The variations in unit-cell dimensions, calculated from the powder patterns, are shown in Fig. 2. The ordinate is kept to the same scale for all three axes. Substitution of palladium for copper causes a rapid increase in the a and b dimensions, but the c dimension contracts slightly. This accounts for the substantial differences in the powder patterns of the two end members. All the experimental evidence indicates that the two compounds are isostructural and completely miscible at ca. 750°C.
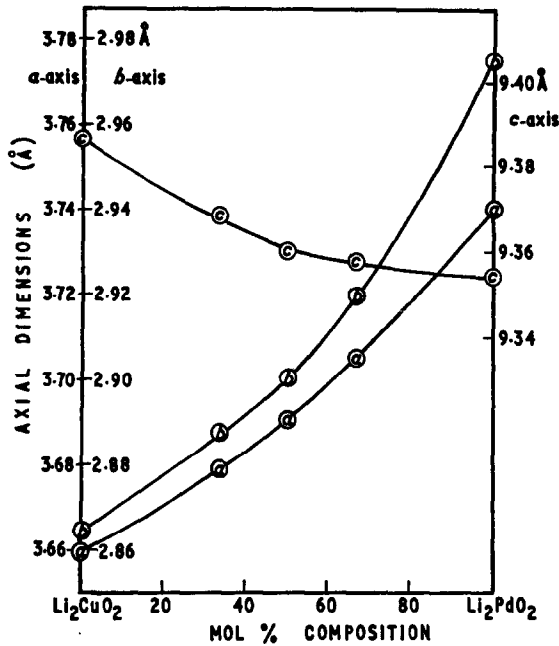
FIG. 2. The unit-cell dimensions of Li_2CuO_2 Li_2PdO_2 and their solid solutions, showing variations with composition.

A structure analysis of Li_2CuO_2 is now in progress, in order to determine bond distances and angles, as they probably differ substantially from those in Li_2PdO_2.

Phase Equilibria in the Li–Pd–O System

Combinations of phases that can coexist at 600°C are shown in Fig. 3. Joins that are shown as continuous lines have been confirmed experimentally; the existence of those joins shown as broken lines is inferred. At 600°C, the oxygen partial pressure necessary to stabilize Li_2PdO_3 is approximately 1 atm, so that a decrease in oxygen pressure causes decomposition to Li_2PdO_2 with liberation of oxygen. Reduction of Li_2PdO_2 yields Li_2O and Pd metal. PdO can coexist with either or both Li_2PdO_3 and Li_2PdO_2;
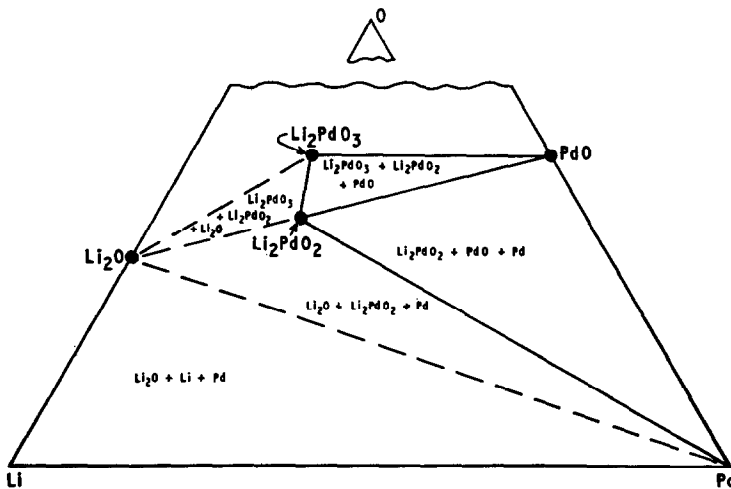

FIG. 3. Phase diagram of the Li–Pd–O system, showing combinations of phases that can coexist in equilibrium at 600°C. Continuous lines represent joins that have been confirmed experimentally; broken lines show joins whose existence is inferred. The oxygen-rich portion has been truncated.

Pd metal can coexist with PdO and Li_2PdO_2 but not with Li_2PdO_3.

At higher temperatures, approx 680–720°C, "Li_2PdO_2" shows some signs of partial melting. This gives rise to a large and reversible heat effect by DTA. It was at first thought that the effect was due to a phase transformation, but a high-temperature X-ray powder pattern failed to reveal any changes in the Li_2PdO_2 phase itself. However, a gradual and progressive increase in the intensities of X-ray reflections attributable to PdO indicated some decomposition, due to slow but cumulative loss of Li_2O during the course of the photographic exposure. A similar loss of lithia occurred during the DTA, although in this case, the loss is primarily due to reaction of the Li_2PdO_2 with the silica sample holder, rather than to volatilization. It is therefore likely that the partial melting observed at $700 \pm 20°C$ commences at a eutectic in the PdO-rich region of the ternary system, or at a binary eutectic on the Li_2PdO_2–PdO join. In experiments where the stoichiometry of the Li_2PdO_2 phase could be more carefully controlled, as in the oxygen-filled sealed tubes, Li_2PdO_2 itself showed no signs of melting or decomposition at temperatures as high as 1050°C.

Acknowledgments

Note added in proof. Since this study was completed we have discovered a report on the preparation and crystal structure of Li_2CuO_2 by R. Hoppe and H. Rieck, *Zeit. Anorg. Allgem. Chem.* **379,** 157 (1970). The same authors have also studied Li_2NiO_2 (ibid, **392,** 193 (1972)). Comparison of the atomic coordinates shows that both Li_2CuO_2 and Li_2NiO_2 are isostructural with Li_2PdO_2.

References

1. J. A. GARD, *in* "The Electron-Optical Investigation of Clays" (J. A. Gard, Ed.), Chap. 2, pp. 40–55. Mineralogical Society, London (1971).

2. W. J. MOORE AND L. PAULING, *J. Amer. Chem. Soc.* **63,** 1392 (1941).

3. H. E. SWANSON, R. K. FUYAT, AND G. M. UGRINIC, *Nat. Bur. Stand. (U.S.) Circ. No. 539* **4,** 27 (1955); Powder Diffraction File, Card No. 6-515. Joint Committee on Powder Diffraction Standards, Swarthmore (1971).

4. H. E. SWANSON, M. C. MORRIS, R. P. STINCHFIELD, AND E. H. EVANS, *Nat. Bur. Stand. (U.S.) Monogr.* **25,** Sec. 1 (1962); Powder Diffraction File, Card No. 12-254. Joint Committee on Powder Diffraction Standards, Swarthmore (1971).

5. J. J. SCHEER, A. E. VAN ARKEL, AND H. BADE, *Can. J. Chem.* **33,** 683 (1959).

6. H. LETZELTER, Dissertation, Karlsruhe (1960); ref. G. LANG, *Z. Anorg. Allg. Chem.* **348,** 254 (1966).

7. J. F. DORRIAN AND R. E. NEWNHAM, *Mater. Res. Bull.* **4,** 179 (1969).

8. W. KLEMM, G. WEHRMEYER, AND H. BADE, *Z. Elektrochem.* **63,** 56 (1959).

9. Powder Diffraction File, Card No. 20-623. Joint Committee on Powder Diffraction Standards, Swarthmore (1971).

10. "International Tables for X-ray Crystallography," Vol. III. Kynoch Press, Birmingham (1962).